Supporting Information

Engineering a Biodegradable Multifunctional Antibacterial Bioactive Nanosystem for Enhancing Tumor Photothermo-Chemotherapy and Bone Regeneration

Yumeng Xue [a, £], Wen Niu [a, £], Min Wang [a], Mi Chen [a], Yi Guo [a, d], Bo Lei [a, b, c *]

[a] *Frontier Institute of Science and Technology, Xi'an Jiaotong University, Xi'an 710000, China*

[b] *Key Laboratory of Shaanxi Province for Craniofacial Precision Medicine Research, College of Stomatology, Xi'an Jiaotong University, Xi'an 710054, China*

[c] *Instrument Analysis Center, Xi'an Jiaotong University, Xi'an 710054, China*

[d] *Department of Biologic and Materials Science, University of Michigan, Ann Arbor, MI, 48109, USA*

[£] *Yumeng Xue and Wen Niu contributed equally to this work.*

**Corresponding author: rayboo@xjtu.edu.cn*

EXPERIMENTAL SECTION

Materials

Dodecylamine (DDA), tetraethyl orthosilicate (TEOS), triethylphosphate (TEP), calcium nitrate tetrahydrate (CN), dopamine (DA), ethyl alcohol (99% ETOH), doxorubicin hydrochloride (DOX) were purchased from Sigma-Aldrich. All chemicals were used as received without further purification.

Antibacterial capacity evaluation

The gram-positive bacteria (S. aureus) and gram-negative bacteria (E. coli) was used to evaluate the antibacterial activity of BGN@PDA nanoparticles. BGN nanoparticles were used as control. The bacterial culture and antibacterial activity analysis were performed according to previous report.[1]

Drug intracellular delivery efficiency

Colon cancer cells (Hct116 cells) were used for the *in vitro* cellular uptake efficiency study. The cellular uptake and distribution of BGN@PDA-DOX in Hct116 cells were demonstrated to study the internalization efficiency of the nanoparticles. Hct116 cells were seeded on the slides and cultured for 24 h until the cells adhered. Then the cells were exposed to BGN@PDA-DOX at a concentration of 50 μg/mL for 6 h, 12 h and 24 h, free DOX (0.5 μg/mL) was used as control. After further incubation, cells were collected and washed with PBS to remove excess materials and media. Then the cells were fixed with 4% paraformaldehyde solutions and Hoechst 33342 (Life Science) were employed to indicate the cell nucleus. Then the fluorescence of cells was observed under the Laser Confocal Microscopy (FV1200, Olympus).

Cytotoxicity and *in vitro* chemotherapy effect

Cells (Hct116 cells/Hela cells)) were seeded in 96-wells cell culture plate at a density of 6000 cells/well and incubated for 24 h. Then the culture medium (McCoy's 5A medium supplemented with 10% Fetal Bovine Serum for Hct116 cells and DMEM supplemented with 10% Fetal Bovine Serum for Hela cells) was replaced

by new medium containing BGN@PDA-DOX, BGN@PDA and DOX with selected concentrations (15, 30, 60, 125 and 250 μg/mL in terms of BGN@PDA) and further incubated at 37 ℃ for another 24 h and 48 h. The cell survival efficiency was measured by using alamar blue kit (Life Science). The fluorescence intensity was tested through a microplate reader at an excitation/emission wavelength of 530/600 nm (SpectraMax@, Molecular Services) to reveal the *in vitro* cytotoxicity of different samples. Moreover, after treated with different samples for 48 h, cells were stained with the Calcein AM fluorescent dye to observed the live cells (Life Science). The morphology and growth states were observed and recorded on an inverted fluorescent microscope (Olympus, IX53). Specifically, Hct116 cells and Hela cells were treated with BGN and BGN@PDA nanoparticles with concentrations up to 1 mg/mL for 48 h to study the cytocompatibility of the nanoparticles. The cell viability was measured by alamar blue kit (Life Science).

***In vitro* biodegradation of BGN@PDA-DOX**

BGN，BGN@PDA and BGN@PDA-DOX were dispersed in different medium (pH=5.5 PBS, pH=7.4 PBS and DMEM+10% FBS) with a concentration of 2 mg/mL and the medium was refreshed every 2 days. TEM images of the nanoparticles were taken at different time (day 2, day 4 and day 8) and ICP analysis of silicon were also conducted at selected time points (day 2, day 14 and day 56) to further evaluate the biodegradation behavior of the nanoparticles as a function of pH, biological media and time.

***In vivo* biodistribution of BGN@PDA-DOX**

Female BALB/c nude mice (5−6 weeks old) were purchased from Xi'an KEAO Biotechnology Co., Ltd. All animal experiments were conducted in compliance with the animal care and use guidelines of National Institutes of Health and the animal research committee of Xi'an Jiaotong University. Hct116 cells (3×10^6) in 100 μL of PBS were subcutaneously injected into the back of each mouse to develop tumor models. To measure the *in vivo* circulation and distribution of BGN@PDA-DOX, tumor-bearing mice were

intravenously injected with BGN@PDA-DOX or free DOX. After 24 h, the mice were sacrificed, the main organs (heart, liver, spleen, lung and kidney) and tumor tissues of the mice were collected and analyzed by an IVIS Spectrum *in vivo* imaging system. Mice treated with PBS were used as control.

***In vivo* long-term biodegradation evaluation**

The long-term biodegradation of BGN@PDA *in vivo* was carried out on ICR mice (female, 4 weeks old). Briefly, the mice of BGN@PDA group and control group (saline) were injected with nanoparticles (20 mg/kg) or saline solution *via* the tail vein. After different times (1 week, 2 week, 4 week, 8 week, 12 week), the mice of various groups were sacrificed, the main organs were removed and fixed for next analysis. The biodegradation of nanoparticles was measured through the Si concentration in various tissues including heart/liver/lung/kidney/brain/spleen. The Si concentration was tested through the ICP analysis. TEM images of the feces of the mice after treated with BGN@PDA for 24 h were taken to further study the degradation and clearance behavior. Moreover, nano titanium dioxide (~200 nm, Aladdin) as one of the most common inert biomaterials for bone tissue engineering was employed as a control for the long-term biodegradation experiments. Specifically, ICR mice (female, 4 weeks old) were injected with BGN@PDA or titanium dioxide (20 mg/kg) *via* tail vein. Mice treated with saline solution was used as control. The mice were sacrificed at predetermined time points (1 week, 2 week and 6 week) and the main organs (heart, liver, spleen, lung and kidney) were collected for ICP analysis of silicon or titanium in different tissues.

***In vivo* photothermal imaging, thermo-chemotherapy and histology analysis**

The tumor model was developed by subcutaneously injection of Hct116 cells (3×10^6) in 100 μL of PBS into the back of each mouse. After the tumor diameter reached 6-8 mm, the mice were randomly divided into six groups (n=6), different groups of mice were subcutaneously injected with 100 μL of fibrin glue mixed with BGN@PDA-DOX, BGN@PDA, DOX and PBS, respectively. Then the mice were anesthetized with chloral

hydrate (10 wt%, 0.3mL/100g) under a rigorous aseptic condition and the tumors were treated with or without NIR laser irradiation (808 nm, 1.4 W/cm^2) for 10 min. The real-time temperature of the tumor tissue was monitored and recorded on a visual IR thermometer when the tumors were exposed to the laser. The body weights and tumor volumes ((tumor length)×(tumor width)^2/2) of the mice were recorded every day. The injection was conducted every two days and NIR irradiation was carried out for three times during the treatment process. Mice in all groups were euthanized on the 12th day and the tumors were dissected. The weight and final volumes of the dissected tumors were recorded. Then the harvested tumor tissues were fixed in 10% formalin, embedded in paraffin, and sectioned into 4 μm slices for hematoxylin and eosin (H&E, Sigma) staining and terminal deoxynucleotidyl transferase-mediated deoxyuridine triphosphate nick end (TUNEL, Sigma) staining. The stained tumor slices were observed under the microscope (Olympus, BX53F) and the images were recorded. The main organs (liver, spleen, kidney, heart, and lung) of the mice were also harvested for H&E staining to study the *in vivo* biosafety of BGN@PDA and side effects of DOX.

***In vitro osteoblastic cell compatibility,* osteogenic differentiation and *in vivo* bone regeneration**

To investigate the *in vitro* osteoblastic cytocompatibility, MC3T3-E1 cells were seeded in 96-wells cell culture plate and incubated for 24 h. Then the culture medium (DMEM supplemented with 10% Fetal Bovine Serum) was replaced by new medium containing BGN@PDA with different concentrations (25, 50, 100, 250, 500 and 1000 μg/mL) and further incubated at 37 °C for another 1 day and 3 days. The cell viability was measured by using alamar blue kit (Life Science). Live/Dead kit was used to visualize the morphology and growth states of cells on an inverted fluorescent microscope (Olympus, IX53). To investigate the influence of thermal effect from NIR irradiation on the bone-related cell behaviors, MC3T3-E1 cells were co-cultured with BGN@PDA nanoparticles at different concentrations with NIR treatment for a period of 3 days and the cell viability was evaluated at different time points. Specifically, after the cells were treated

with BGN@PDA nanoparticles (30, 60, 90 and 200 μg/mL) and cultured for 12 h, NIR was applied to irradiate each well of cells for 10 min. Then the cells were further cultured for 1 day and 3 days. The cell viability and proliferation behavior of cells were investigated by alamar blue kit and Live/Dead Kit.

For the study of osteogenic differentiation of cells, MC3T3-E1 cells were seeded into 24-well plates and treated with various concentrations (30, 60 and 90 μg/mL) of BGN or BGN@PDA nanoparticles. After incubation for 7 days or 14 days, cells were collected and the cell lysates were analyzed for Alkaline phosphatase (ALP) activity using a SensoLyte pNPP ALP assay kit (AnaSpec, Fremont, CA, USA). ALP activity was normalized to total protein content measured using the Pierce BCA protein assay kit (Thermo Fisher Scientific) according to manufacturer instructions. The levels of ALP activity were determined from absorbance at 405 nm using a microreader.

Moreover, qRT-PCR analysis was conducted to evaluate the expression of osteogenic markers Runx2 and Bsp. Cells were treated with BGN or BGN@PDA (60 μg/mL) for 7 days or 14 days. Then the total RNA was extracted from MC3T3-E1 cells and single-stranded cDNAs were prepared from 0.5 μg RNA by using a RevertAid firststrand cDNA synthesis kit (Roche). The cDNA and SYBR green Master Mix were added to each well of the array plate. The qRT-PCR (Applied Biosystems 7500; Bio-rad) was performed by using the following parameters: heated from room temperature to 95 °C for 2 min, and cycled 40 times at 95 °C for 15 s, then cooled down from 95 °C to 60 °C for 1 min. The primers for qRT-PCR are displayed in Table S2. The expression of osteogenic genes (Runx2 and Bsp) and ALP activity of MC3T3-E1 cells on day 7 and day 14 were also test after the cells were co-cultured with BGN@PDA nanoparticles for 12 h and treated with NIR irradiation for 10 min to further study the effect of NIR treatment on cells behavior. The bone regeneration capacity of BGN@PDA was studied by a rat cranial critical sized defect model (Sprague Dawley rats, 6 weeks, male, 200-220 g). Typically, the rats were anesthetized with chloral hydrate (10 wt%,

0.3mL/100g) and two defects with a diameter of 5 mm were made on the calvarium of each rat. Fibrin glue (Porcine Fibrin Sealant Kit, Hangzhou puji Pharmaceutical technology development co., LTD) were mixed with BGN@PDA or BGN to form injectable hydrogel complexes in the defect site to immobilize the nanoparticles during the implantation process and the pure fibrin glue was used as blank. Rats in all groups were sacrificed after 4 weeks and the calvarium of each rat were harvested for microCT (Y.CHEETAH*, YXLON) investigation and histological study. Before the histology evaluation, the bone samples were immersed in 10% EDTA for decalcifying, embedded in paraffine and sectioned in to 5 μm slices. After stained with hematoxylin and eosin (H&E, Sigma) and masson's trichrome (Sigma), the slices were observed under the microscope and the images were recorded on the computer. Additionally, the *in vivo* bone repair efficacy of BGN@PDA nanoparticles combine with NIR treatment was evaluated to study the thermal effect on the bone regeneration process. Typically, after the implantation of BGN@PDA nanoparticles, the implantation sites were irradiated by NIR laser once a week. The rats were sacrificed after 4 weeks-treatment and the defects tissues were collected for microCT analysis.

Statistical analyses

All data are expressed as the mean ± standard deviation (SD). All statistical analyses were performed with SPSS software (version 17.0). Significant differences between two groups were determined by Student's t test. *$P < 0.05$ was considered statistically significant. All experiments were performed at least in triplicate.

SUPPORTING FIGURES

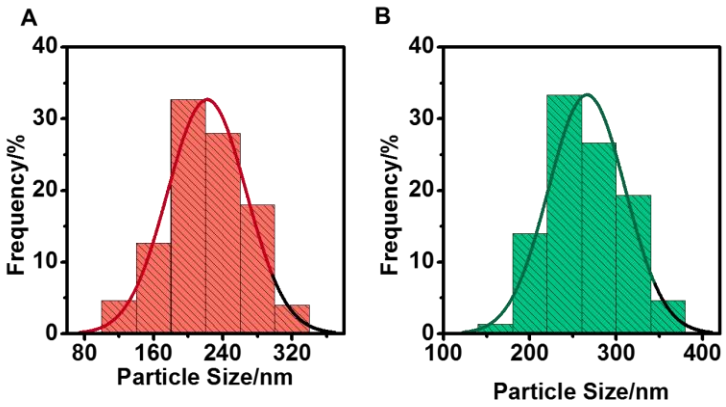

Figure S1. Size distribution of (A)BGN and (B)BGN@PDA based on TEM images.

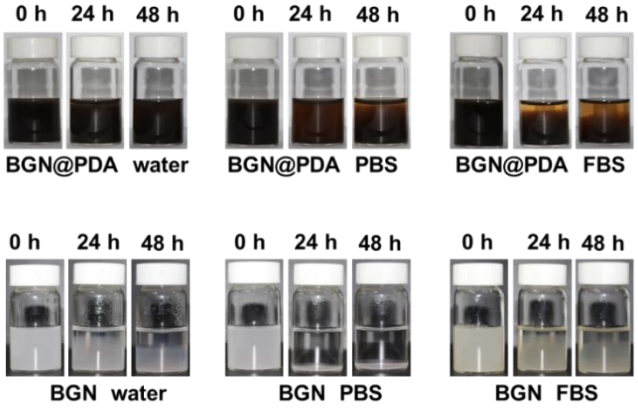

Figure S2. Physiological stability evaluation. Digital images of BGN@PDA and BGN dispersed in water, PBS and FBS solution (10%) for 48 h.

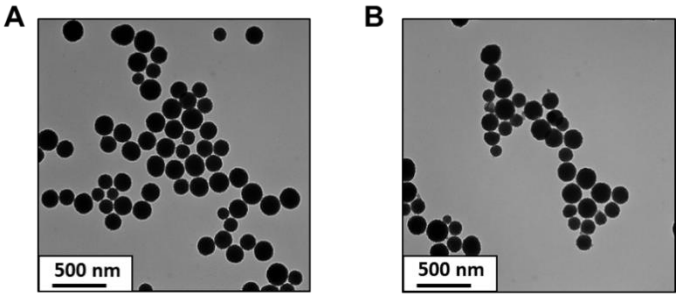

Figure S3. TEM images of (A)BGN and (B)BGN@PDA after NIR irradiation for 10 min.

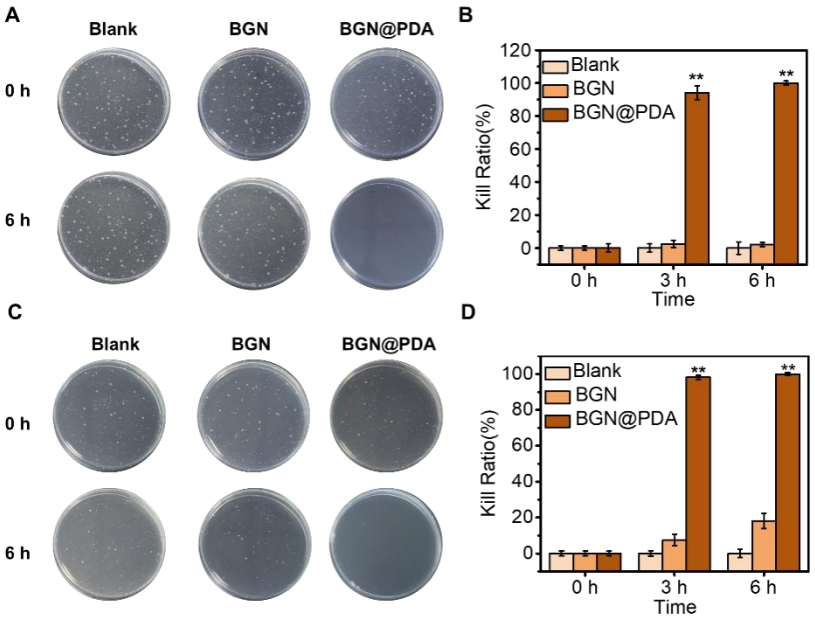

Figure S4. Antibacterial activity of BGN@PDA nanoparticles. (A) *In vitro* growth inhibition of E. coli bacteria on agar plate and (B)the corresponding bacteria kill ration after incubated for 6 h; (C) *In vitro* growth inhibition of S. aureus bacteria on agar plate and (D)the corresponding bacteria kill ration after incubated for 6 h. *p < 0.05; **p < 0.01.

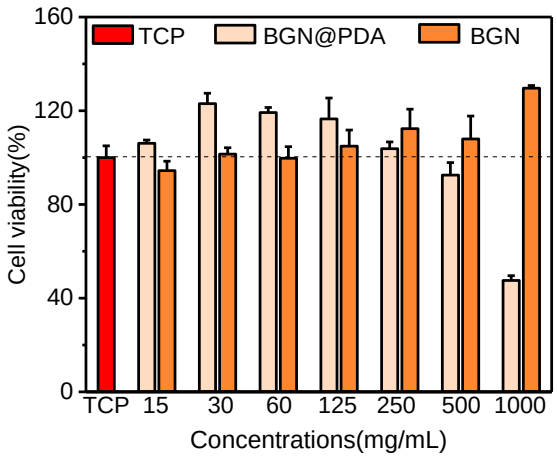

Figure S5. Cytocompatibility evaluation of BGN and BGN@PDA nanoparticles against Hct116 cells for 48 h with different concentrations.

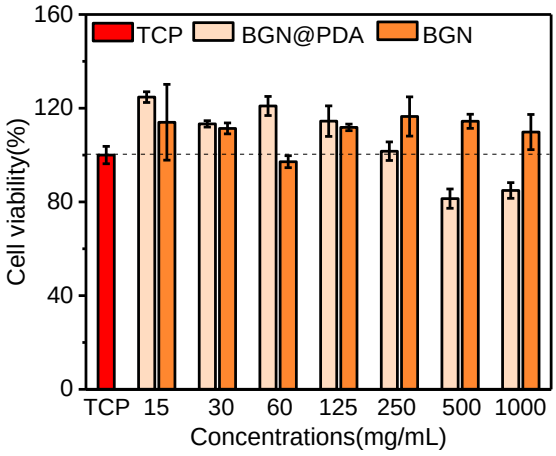

Figure S6. Cytocompatibility evaluation of BGN and BGN@PDA nanoparticles against Hela cells for 48 h with different concentrations.

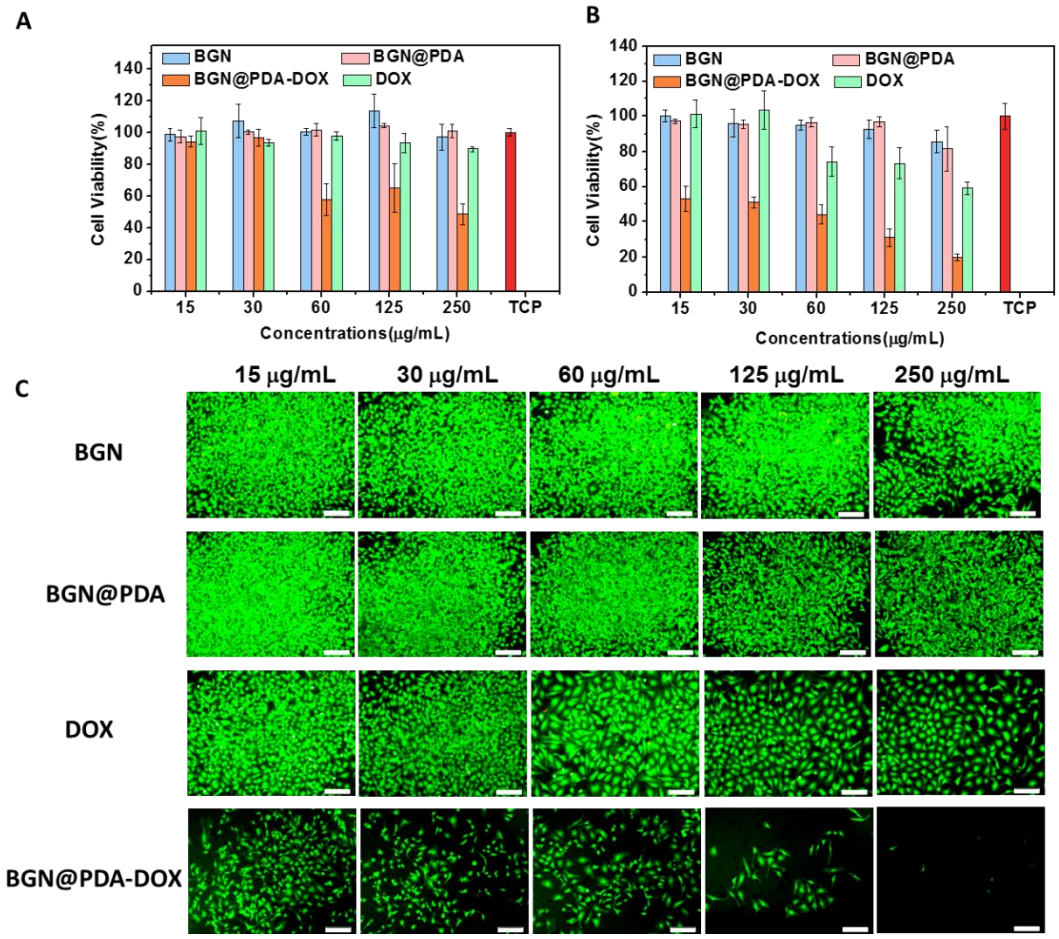

Figure S7. Cell viability of HeLa cells after incubation with BGN, BGN@PDA, BGN@PDA-DOX and DOX at various concentrations for (A)24 h and (B)48 h. (C)Images of Hela cells after incubated with BGN, BGN@PDA, BGN@PDA-DOX and DOX at various concentrations for 48 h (Scale bars: 200 μm).

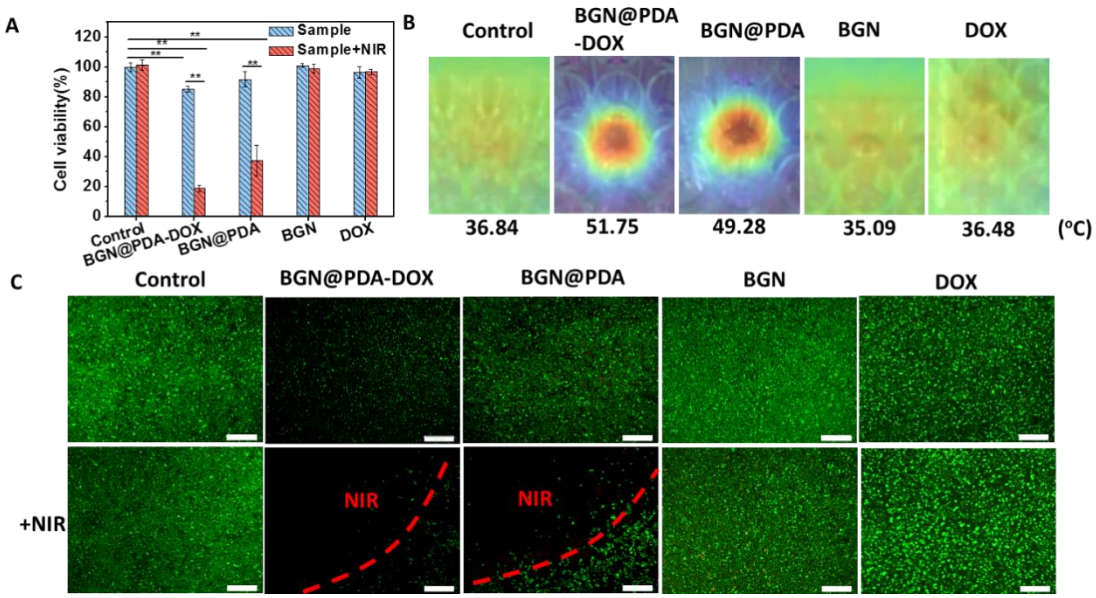

Figure S8. In vitro chemo- and photothermal therapy efficiency. (A)Cell viability of Hela cells after treated with BGN, BGN@PDA, BGN@PDA-DOX and DOX at a same DOX concentration level ((in terms of BGN or BGN@PDA: 200 μg/mL, DOX : 2.5 μg/mL) with or without the treatment of laser; (B)Infrared thermal imaging of a 48-well cell-culture plate containing Hela cells which co-cultured with BGN@PDA-DOX BGN@PDA, BGN and DOX under 808 nm NIR irradiation for 10 min (808 nm, 1.4 W/cm^2); (C)Images of live Hela cells incubated with BGN@PDA-DOX, BGN@PDA, BGN and DOX and treated with 808 nm laser (1.4 W/cm^2) for 10 min (Scale bars: 500 μm).

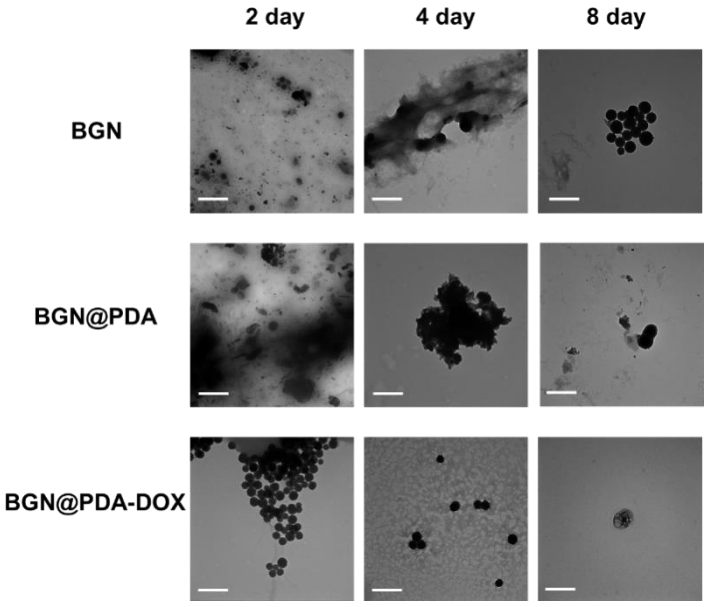

Figure S9. TEM images of BGN, BGN@PDA and BGN@PDA-DOX in PBS (pH=5.5) for 8 days (Scale bar: 500 nm).

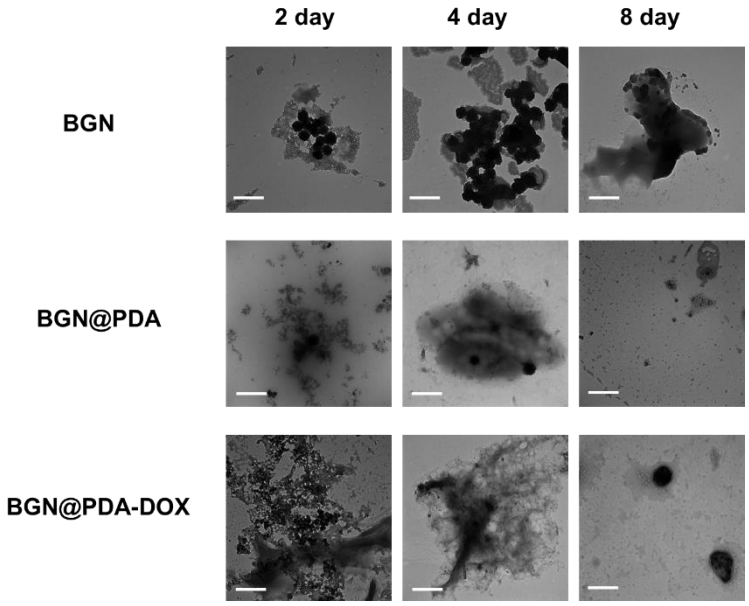

Figure S10. TEM images of BGN, BGN@PDA and BGN@PDA-DOX in PBS (pH=7.4) for 8 days (Scale bar: 500 nm).

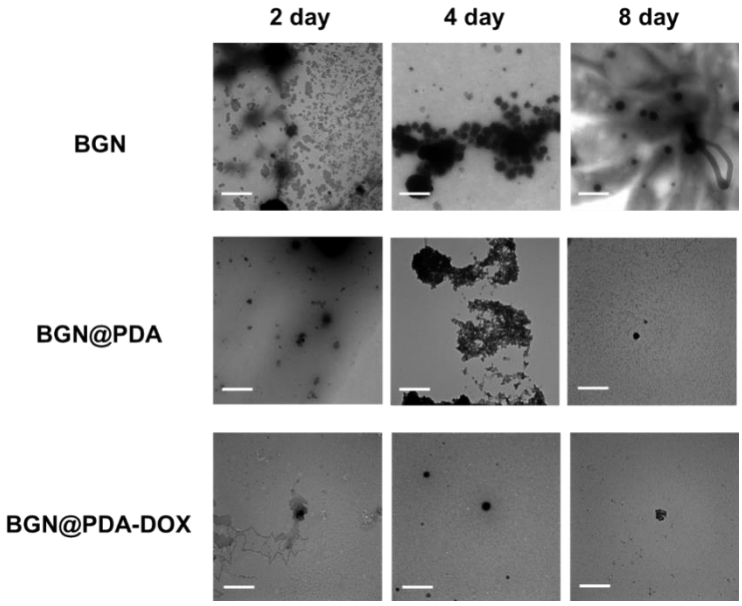

Figure S11. TEM images of BGN, BGN@PDA and BGN@PDA-DOX in serum solutions (DMEM+10% FBS) for 8 days (Scale bar: 500 nm).

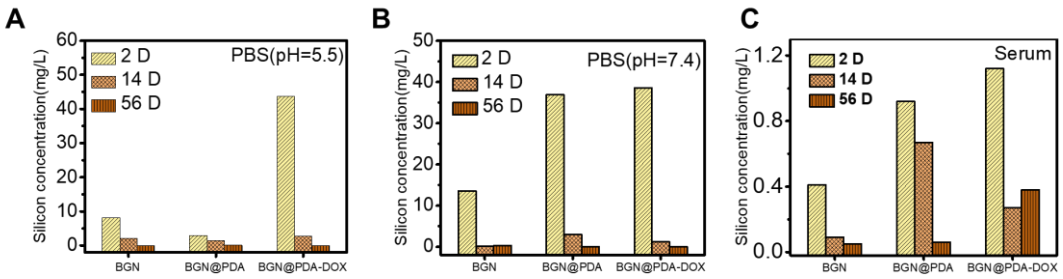

Figure S12. ICP analysis of the silicon released concentration from BGN, BGN@PDA and BGN@PDA-DOX in (A)pH=5.5 PBS, (B) pH=7.4 PBS and (C) serum solutions (DMEM+10%FBS) at selected time points.

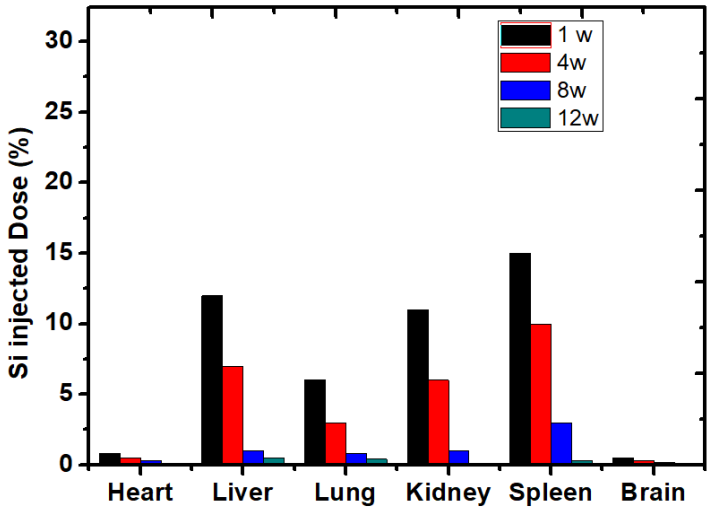

Figure S13. Biodegradation and biodistribution of Si in main organs after intravenous injection of BGN@PDA in mice for 1 w, 4w, 8w, 12 w.

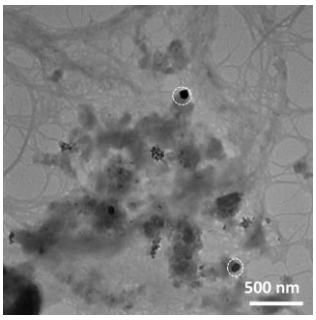

Figure S14. TEM images of the feces of mice after treated with BGN@PDA for 24 h.

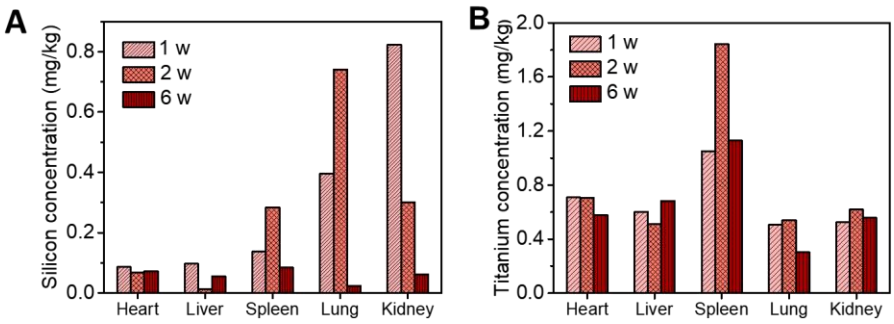

Figure S15. Biodegradation and biodistribution of Silicon and Titanium in main organs after intravenous injection of (A)BGN@PDA and (B)nano titanium dioxide in mice for 1 w, 2w and 6 w.

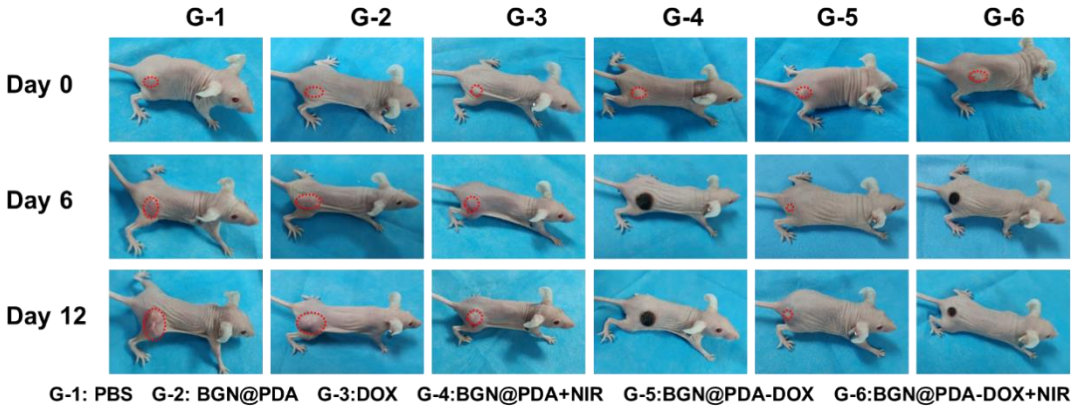

Figure S16. Digital images of mice in different group during the treatment process.

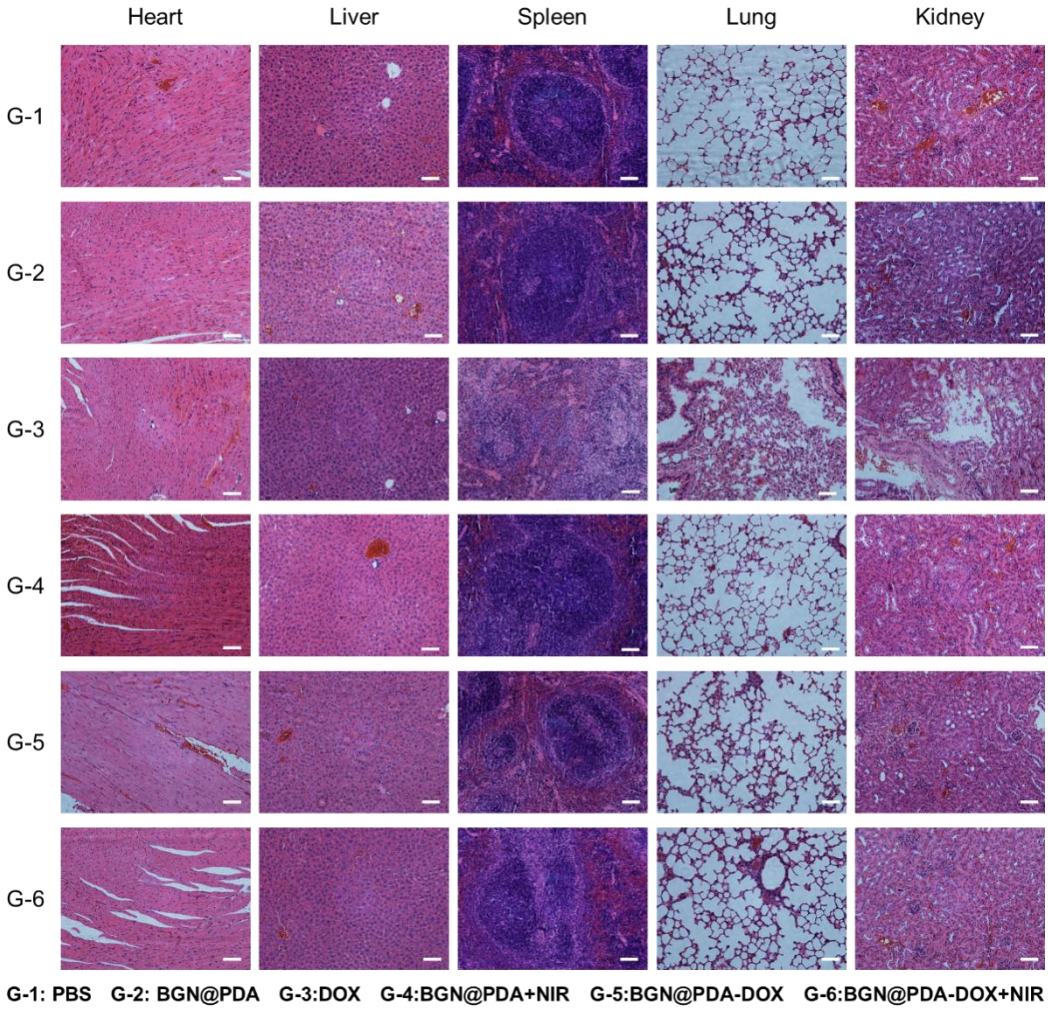

Figure S17. H&E staining images of the main organs in different treatment groups (Scale bars: 50 μm).

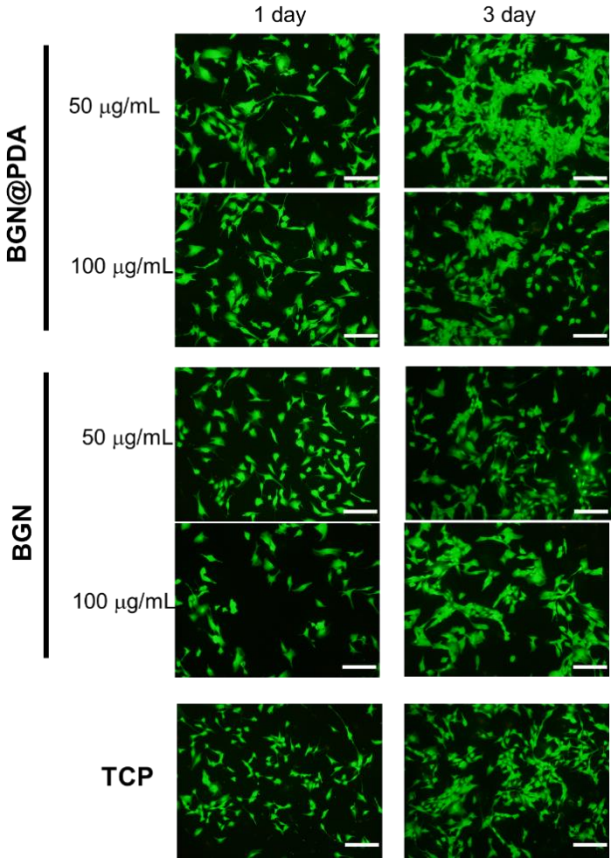

Figure S18. Fluorescent images of MC3T3-E1 cells after co-culturing with BGN and BGN@PDA with concentrations of 50 and 100 μg/mL for 1 day and 3 days (Scale bars: 200 μm).

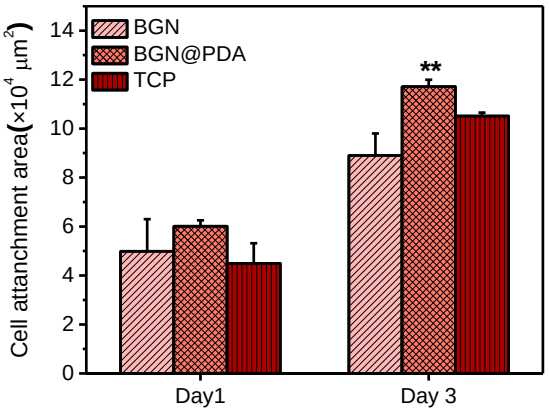

Figure S19. Quantification of cell attachment area based on the fluorescent images of MC3T3-E1 cells after treated with BGN or BGN@PDA for 3 days with concentration of 50 μg/mL.

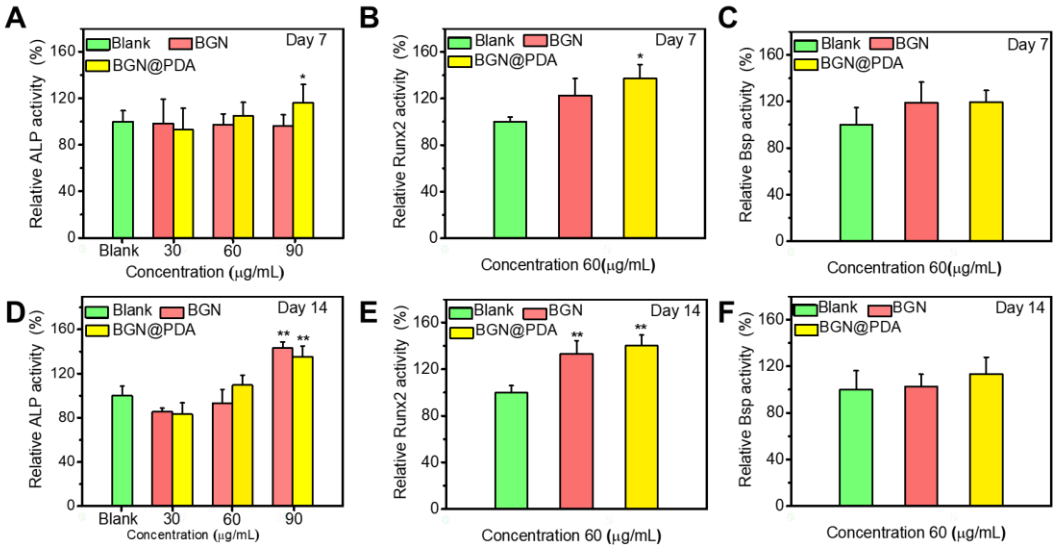

Figure S20. ALP activity analysis and osteoblastic marker-gene expressions during osteogenic differentiation following co-culturing with BGN or BGN@PDA nanoparticles for 7 days and 14 days. (A)(D) ALP activity evaluation and expression levels of (B)(E) Runx2 and (C)(F) Bsp on (A-C) day 7 and (D-F) day 14. *p < 0.05; **p < 0.01. All experiments were performed in triplicate (n = 5 per group).

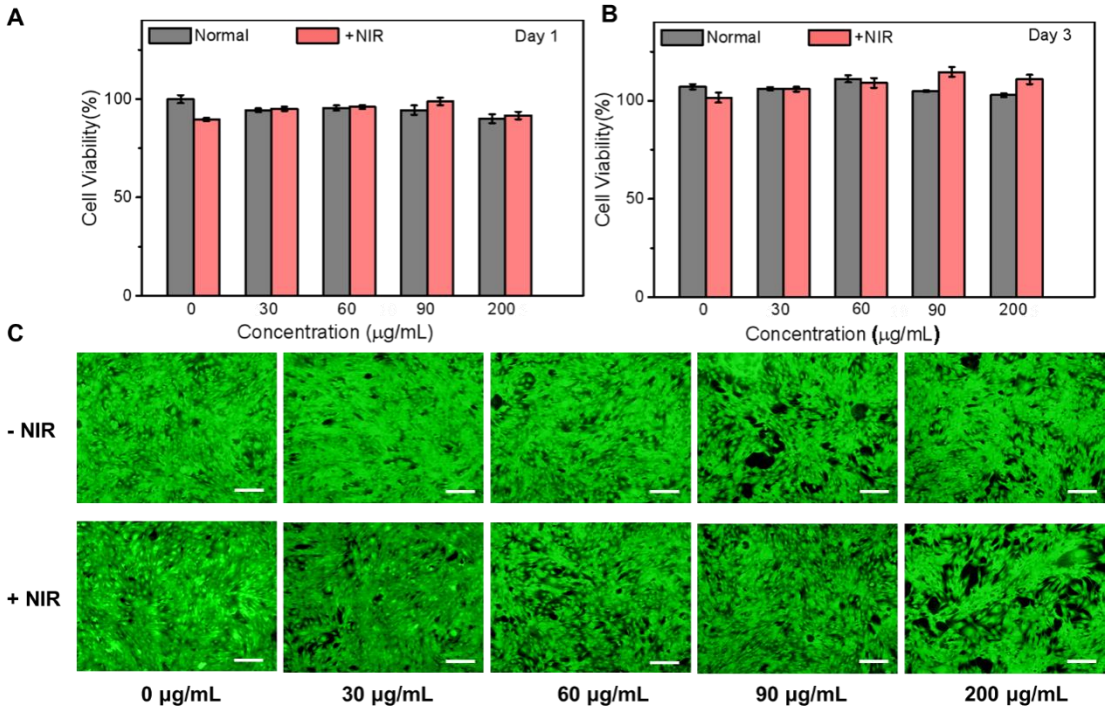

Figure S21. The influence of NIR irradiation on the cell growth and proliferation. The cell viability of MC3T3-E1 cells after treated with BGN@PDA nanoparticles at different concentrations with or without NIR irradiation for (A)1 day and (B)3 days; (C) The fluorescent images of MC3T3-E1 cells after co-cultured with BGN@PDA for 3 days with or without NIR irradiation (Scale bars: 200 μm).

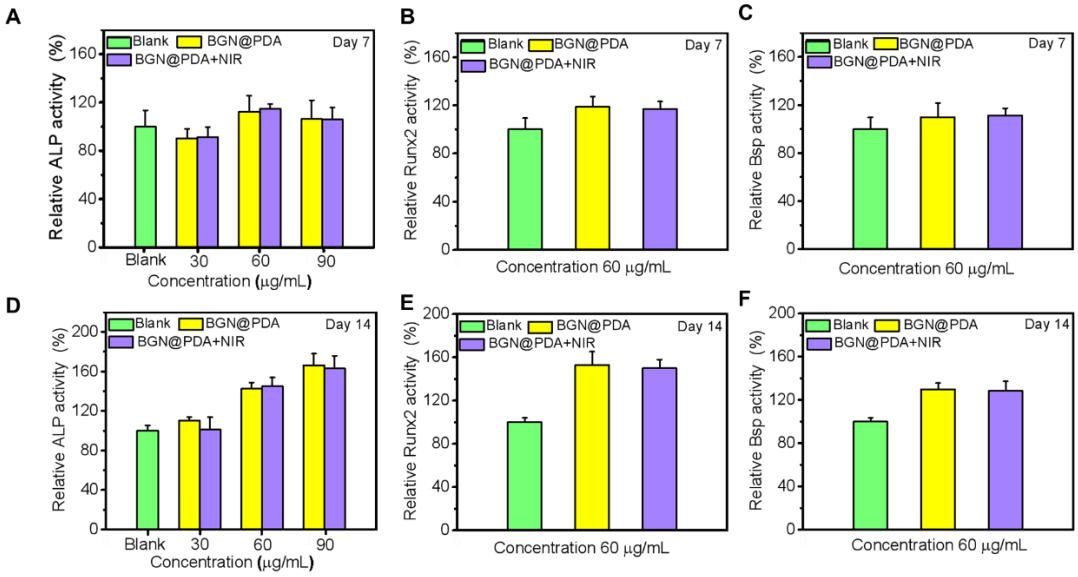

Figure S22. Osteoblastic marker-gene expressions during osteogenic differentiation following co-culturing with BGN@PDA nanoparticles for 7 days and 14 days with or without NIR irradiation. Expression levels of (A)(D) ALP, (B)(E) Runx2 and (C)(F) Bsp evaluation on (A-C) day 7 and (D-F) day 14. All experiments were performed in triplicate (n = 5 per group).

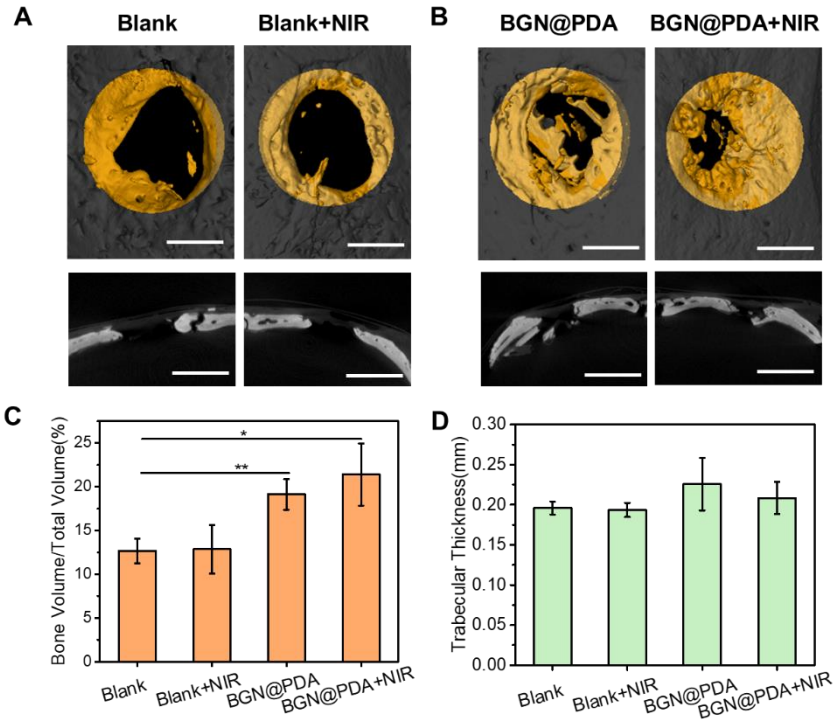

Figure S23. (AB)MicroCT images of the cranial defects after implanting with BGN@PDA for 4 weeks with or without NIR irradiation (Scale bars: 2 mm); Quantitative analysis of (C) new bone volume fraction and (D)trabecular thickness calculated based on micro-CT analysis.

Table S1 DLS analysis of BGN and BGN@PDA before and after NIR irradiation

	Mean hydrodynamic diameter (nm)
BGN	159.2
BGN+NIR	134.9
BGN@PDA	262.2
BGN@PDA+NIR	237.4

Table S2 Real-time PCR primers

Genes	Forward primer (5'-3')	Reverse primer (5'-3')
Runx2	TCTTCCCAAAGCCAGAGCG	TGCCATTCGAGGTGGTCG
Bsp	CAGGTGAAGGAGAGAGCGTC	CACTAGGAGCGGTGGTTGTC

REFERENCES

(1) Li, Y.; Li, N.; Ge, J.; Xue, Y.; Niu, W.; Chen, M.; Du, Y.; Ma, P. X.; Lei, B., Biodegradable Thermal Imaging-Tracked Ultralong Nanowire-Reinforced Conductive Nanocomposites Elastomers with Intrinsically Efficient Antibacterial and Anticancer Activity for Enhanced Biomedical Application Potential. *Biomaterials*, **2019**, *201*, 68-76.